Estimating Daclizumab effects in Multiple Sclerosis using Stochastic Symmetric Nets

Pernice Simone
Department of Computer Science,
University of Torino,
Torino, Italy
pernice@di.unito.it

Beccuti Marco
Department of Computer Science,
University of Torino,
Torino, Italy
beccuti@di.unito.it

Do' Pietro
Department of Life Sciences and Systems Biology,
University of Torino,
Torino, Italy
pietro.do_@edu.unito.it

Pennisi Marzio
Department of Mathematics and Computer Science,
University of Catania,
Catania, Italy
mpennisi@dmi.unict.it

Pappalardo Francesco
Department of Drug Sciences,
University of Catania,
Catania, Italy
francesco.pappalardo@unict.it

***Abstract*—Multiple Sclerosis (MS) is an immune-mediated inflammatory disease of the central nervous system which damages the myelin sheath enveloping nerve cells causing severe physical disability in patients. Relapsing Remitting Multiple Sclerosis (RRMS) is one of the most common form of MS and it is characterized by a series of attacks of new or increasing neurologic symptoms, followed by periods of remission. Recently, many treatments were proposed and studied to contrast the RRMS progression. Among these drugs Daclizumab, an antibody tailored against the interleukin-2 receptor of T cells, exhibited promising results. Unfortunately, more recent studies on Daclizumab highlight severe adverse effects, that led to its retirement from the EU marketing authorization process. Motivated by these recent studies, in this paper we describe how computational modelling can be efficiently exploited to improve our understanding on Daclizumab mechanism of action, and on how this mechanism leads towards the observed undesirable effects.**

***Index Terms*—Multiple sclerosis, Computational modelling, Uncertainty Analysis, Sensitivity Analysis**

I. Introduction

Multiple sclerosis (MS) is a chronic and potentially highly disabling disease with considerable social impact and economic consequences. In Europe it is the leading cause of non-traumatic disabilities in young adults, since more than 700,000 EU people suffer from MS [1]. Practically, in MS the immune system attacks the myelin, a fatty substance which isolates and protects the axons in the nervous system. This damage disrupts the ability of the nervous system to communicate, resulting in a range of signs and symptoms which can cause physical disability within 25 years in more than 30% of patients [2].

In literature four courses of MS are identified: Relapsing-Remitting MS (RRMS), Secondary Progressive MS (SPMS), Primary Progressive MS (PPMS), and Progressive Relapsing MS (PRMS). Among them the RRMS is the most common course since it is diagnosed in about 85% of MC cases. It is characterized by long periods of stability (i.e. remissions) interrupted by episodes of neurological dysfunction (i.e. relapses) followed by a complete or partial recovery. Moreover, within 25 years RRMS usually changes to SPMS (in about 90% of cases) increasing the disease severity. [1]

In the last two decades the advances in the understanding of the immune pathogenesis of MS and the advent of Monoclonal Antibodies (mAb) allowed researchers to define novel treatments against this disease. In particular mAb are powerful new tools to modify the course of MS based on a molecular targeted approach. Indeed they are potentially able to break the immune cascade of events that brings to the autoimmune reaction causing the myelin loss. Therefore, these treatments that include several mAbs such as Natalizumab, Rituximab and Alemtuzumab, constitute nowadays the most effective first and second line treatments in the therapy of MS [3]–[5].

Moreover, when the first and second line treatments provided an inadequate response in patients, Daclizumab treatment [6] represented the only third line treatment to be used as a valid alternative. Differently from the other mAbs, Daclizumab is a humanized monoclonal IgG1 antibody tailored against InterLeukin-2 Receptor (IL-2R) thus able to break the autoimmune reaction by suppressing the T-cells expansion.

Despite its promising results, in 2018 Daclizumab was retired from the EU marketing authorization process due to the observation of twelve cases of patients who developed, after the start of the treatment, serious immune-mediated adverse reactions at the level of the central nervous system, including encephalitis and meningoencephalitis.

New studies are then needed to better characterize Dacluzumab mechanisms of action, and how these can lead towards the observed undesirable effects. In this paper we present how computational modelling can be exploited to deal with this goal.

Hence, we firstly describe how High Level Petri Net (HLPN) formalism can be efficiently used to derive a graphical and parametric description of the system under study. Then, we show how the ODE system, that can be automatically

978-1-5386-5488-0/18/$31.00 ©2018 IEEE

Authorized licensed use limited to: University of Catania. Downloaded on June 19,2020 at 08:35:03 UTC from IEEE Xplore. Restrictions apply.

derived from HLPN model, mimics the simulated system and how uncertainty and sensitivity analysis can be used to make more robust the results carried out through the model. In details, three sets of experiment are thus reported. In the first experiment the input parameters of model are studied to clear characterize the difference between the behaviour of healthy and ill patients. Then two cases of different RRMS severity are considered for studying the effect of different Daclizumab administration strategies.

In conclusion, this work is the first attempt in which computational modelling is exploited to investigate the effect of Daclizumab drug on RRMS. Indeed, to the best of our knowledge, many previous computational modelling works on RRMS [7], [8] are solely focused on the study of its mechanisms.

II. Background

In this section we intuitively introduce the formalism used to model and analyze our case study. Thus Petri Net formalism is firstly introduced, then its high-level extension called Stochastic Symmetric Net (SSN) [9] is described. Then we report a discussion on how the quantitative properties of a system modelled through such a formalism can be efficiently computed using fluid approximation. In the last part of this section we describe how the model sensitivity analysis can be carried out using a sampling-based method.

A. Stochastic Symmetric Net

Petri Net (PN) [10] and their extensions are well-known computational and mathematical formalisms which provide a graphical intuitive and formal description of the important features of the system under studying. Moreover they allow the using of several different analysis techniques to derive the qualitative and the quantitative properties of a system.

In detail, PNs are bipartite directed graphs with two types of nodes namely places and transitions. Places, correspond to the state variables of the system and they are graphically represented as circles. For instance in Fig. 1 some of model places are the *Treg* and *Teff* representing two typologies of T-cells or the *EBV* modelling the presence of the Epstein-Barr Virus in the system.

Differently, transitions correspond to the events that can induce a state change and they are graphically represented as boxes. For instance in Fig. 1 two transitions are *TeffkillsEBV* to simulate the elimination of the virus by the Teff cells, or *TregKillsTeff* representing the control of the Treg over the Teff cells.

The arcs connecting places to transitions and vice-versa express the relation between states and event occurrences. Places can contain tokens, drawn as black dots. The state of an PN, called *marking*, is defined by the number of tokens in each place.

The system evolution is given by the firing of an enabled transition, where a transition is enabled if and only if each input place contains a number of tokens greater or equal than a given threshold defined by the cardinality of the corresponding input arc. Thus, the firing of an enabled transition removes a fixed number of tokens from its input places and adds a fixed number of tokens into its output places (according to the cardinality of its input/output arcs).

Among PN extensions proposed in literature, Stochastic Symmetric Net (SSN) [9] extends PN providing a more compact and readable representation of the system thanks to the possibility of having distinguished colored tokens, which can be graphically represented as dots of different colors.

In SSN each place p has an associated color domain (a data type) denoted $cd(p)$ and each token in a given place has an associated value defined by $cd(p)$. Color domains are defined by the Cartesian product of elementary types called *color classes* $\mathcal{C} = \{C_1, \ldots, C_n\}$, so that $cd(p) = C_1^{e_1} \times C_2^{e_2} \times \ldots \times C_n^{e_n}$ where e_i is the number of times C_i appears in $cd(p)$. In our model represented in Fig. 1 a color class is the age class, named *Age*, representing the age of a specific token. Then the color domain *cd(Teff)* of the place named *Teff* is defined by the age class and by the position classes ($Age \times PosX \times PosY$). Color classes are finite and disjoint sets. They can be ordered (in this case a successor function is defined on the class, inducing a circular order among the elements in the class), and can be partitioned into (static) subclasses (e.g $C_{i,j}$ is the i^{th} static subclass of color class j^{th}). For instance in Fig. 1 the color class Age is divided in three subsclasses: young (Yo), adult (Ad) and old (Ol).

Similarly a color domain is associated with transitions and it is defined as a set of typed variables where the variables are those appearing in the functions labeling the transition arcs and their types are the color classes. For instance the color domain of transition representing the death of a Teff cell, named *TeffDeath*, is $Age \times PosX \times PosY$ and the variables characterizing its arc are $a \in Age,\ x \in PosX$ and $y \in PosY$.

An instance of a given transition t is an assignment of the transition variables to a specific color of proper type. Hence, we use the notation $\langle t, \mathbf{c} \rangle$ to denote an instance, where $\mathbf{c}$ is the assignment, also called binding. Moreover, a guard can be used to define restrictions on the allowed instances of a transition. It is a logical expression defined on the color domain of the transition, and its terms, called basic predicates allow one (I) to compare colors assigned to variables of the same type ($x = y,\ x \neq y$); (II) to test whether a color element belongs to a given static subclass ($x \in C_{i,j}$); (III) to compare the static sub-classes of the colors assigned to two variables ($d(x) = d(y), d(x) \neq d(y)$).

Each arc connecting a place p to a transition t, namely input arc, is labeled with an expression defined by the function $I[p,t] : cd(t) \rightarrow Bag[cd(p)]$, where $Bag[A]$ is the set of multisets built on set A, and if $b \in Bag[A] \wedge a \in A$, $b[a]$ denotes the multiplicity of a in the multiset b. Similarly each arc connecting a transition t to a place p, namely output arc, is denoted by the function $O[p,t] : cd(t) \rightarrow Bag[cd(p)]$. Thus, the evaluation of $I[p,t]$ (resp. $O[p,t]$) given a legal binding of t provides the multiset of colored tokens that will be withdrawn from (input arc) or will be added to (output arc) the place

Authorized licensed use limited to: University of Catania. Downloaded on June 19,2020 at 08:35:03 UTC from IEEE Xplore. Restrictions apply.

connected to that arc by the firing of such transition instance.

In details, a transition instance $\langle t, \mathbf{c} \rangle$ is enabled and can fire in an marking m iff: (1) its guard evaluated on $\mathbf{c}$ is true; (2) for each place p we have that $I[p,t](\mathbf{c}) \leq m(p)$ where $\leq$ is comparison operator among multisets. We use the notation $E(t,m)$ to denote the set of all instances of t enabled in the marking m. The firing of the enabled transition instance $\langle t, \mathbf{c} \rangle$ in m produces a new marking m' for each place p we have that $m'(p) = m(p) + O[p,t](\mathbf{c}) - I[p,t](\mathbf{c})$.

In the SSN the firing of each transition is assumed to occur after a random delay (firing time) from the time it is enabled. Thus, these stochastic firing delays, sampled from a negative exponential distribution, allows us to automatically derived the stochastic process, i.e. a Continuous Time Markov Chain (CTMC), that mimics the dynamic of SSN model. In detail, the CTMC states are identified with SSN markings and the state changes correspond to the marking changes in the model. In this work we assume that all the transitions of the SSN follow a mass action law so the intensity of $\langle t, c \rangle$ in marking m is defined as follows:

$$\varphi(m,t,\mathbf{c}) = \omega(t,\mathbf{c}) \prod_{\langle p_j,c\rangle : I[p_j,t](\mathbf{c})[c] \neq 0} m[p_j][c]^{I[p_j,t](\mathbf{c})[c]}$$

where $m[p][c]$ denotes the marking of place p for color c, and $\omega(t,\mathbf{c})$ is a function returning the rate of transition t assuming the firing of the instance $\langle t, \mathbf{c} \rangle$.

In the literature, different techniques are proposed to solve this underlying CTMC; in particular, in case of very complex models, the so-called deterministic approach [11] can be efficiently exploited. According to this, in [12] we described how to derive a deterministic process, described through an ODEs system, which well approximates the stochastic behavior of an SSN model. In particular for each place p and possible color tuple $c \in cd(p)$ we have the following ODE equation:

$$\frac{dx_{p,c}(\nu)}{d\nu} = \sum_{\langle t',\mathbf{c}\rangle \in E(t',x(\nu)) \wedge t' \in T} \varphi(x_{p,c}(\nu), t', \mathbf{c})(O[p,t'](\mathbf{c})[c] - I[p,t'](\mathbf{c})[c]) \quad (1)$$

where $x_{p,c}(\nu)$ is the average number of tokens of color c in the place p at time ν, while T is the set of the net transitions.

B. Sensitivity analysis

Sensitivity analysis is broadly used in the computational modelling to study which parameters are important in contributing to model outcome variability. In literature several approaches were proposed to achieve this task, such as Pearson correlation coefficient (CC) method (for linear relationships), Partial Rank Correlation Coefficient (PRCC) method (for non-linear and monotonic relationships) or Fourier Amplitude Sensitivity Test (FAST) method (for any non-linear relationships) [13], [14]. In this work we focus on a sampling-based method which combines Latin Hypercube Sampling (LHS) [15] with PRCC index. Practically LHS, a well-known stratified sampling methods, is adopted to generate samples of the model input variables. Then the model is run N times in a chosen interval: one for each generated input variable sample combination. Finally PRCC between the generated input variables and the obtained model outputs are evaluated on the same chosen interval. In this way PRCC analysis and corresponding significance tests (i.e significant p-value) are used to identify key model parameters and to select time points which need an in-depth study. Specifically, PRCC values close to 1 (-1) identify positive (negative) monotone relationships between inputs and outputs; while the significance tests allow one to discover those correlations that are important, despite having relatively small PRCC values.

III. Relapsing-Remitting Multiple Sclerosis Model

Multiple sclerosis, as already pointed out in the introduction, is a disease that causes the removal of fatty myelin sheath from axons of the central nervous system. RRMS is the predominant type of MS in which the disease alternates periods of active neural inflammation and disease worsening (relapses) to periods of remission. During relapses, the disease worsening may lead to the development and recurrence of symptoms. The occurrences of the relapses periods vary from mild to severe, according to the course and history of the disease. The occurrence and severity of relapses are the only yardstick to estimate the efficacy of a treatment with a specific drug.

In this scenario, T lymphocytes (T-cells) play a central role in disease progression, since they attack the myelin sheaths of axons. In literature, it has been hypothesized that homeostasis of regulatory T cells (Treg) and effectors T cells (Teff) may be crucial to prevent autoimmunity. In particular, a breakdown of the peripheral tolerance mechanisms of Treg (represented, for example, by a lower duplication rate of Treg compared to Teff) can bring to a negative effect in the selection of self-reactive Teff cells, leading to damage in the central nervous system.

The logic implemented into the model is presented as follows and basically recalls to mind a modified Predator-Prey scenario. Due to some genetic predisposition, resting effector T cells and regulatory T cells surpass the thymus selection and become part of the immune system machinery. Once activated, Teff cells can potentially react against myelin based protein epitopes on oligodendrocytes (ODC) producing neural damage. Activation is caused by an external trigger, i.e. the Epstein-Barr Virus (EBV) latent infection, that can lead to autologous lymphocyte activation through a process called molecular mimicry. Mimicry leads EBV epitopic sequences to match the receptors of the autologous T cells that are potentially reactive for the myelin based protein sequences. Activated Teff cells can then attack the myelin in the brain and will be stimulated to duplicate, while activated Treg will work to deactivate active Teff receiving, as a consequence of that, the stimulus to duplicate. Such stimuli are driven by the presence of Interleukin-2 (IL-2), an immunomodulating cytokine released in our model by the T cells themselves in order to self-stimulate their actions. Moreover, IL-2 brings to the activation of another family of cells belonging to the innate

Authorized licensed use limited to: University of Catania. Downloaded on June 19,2020 at 08:35:03 UTC from IEEE Xplore. Restrictions apply.

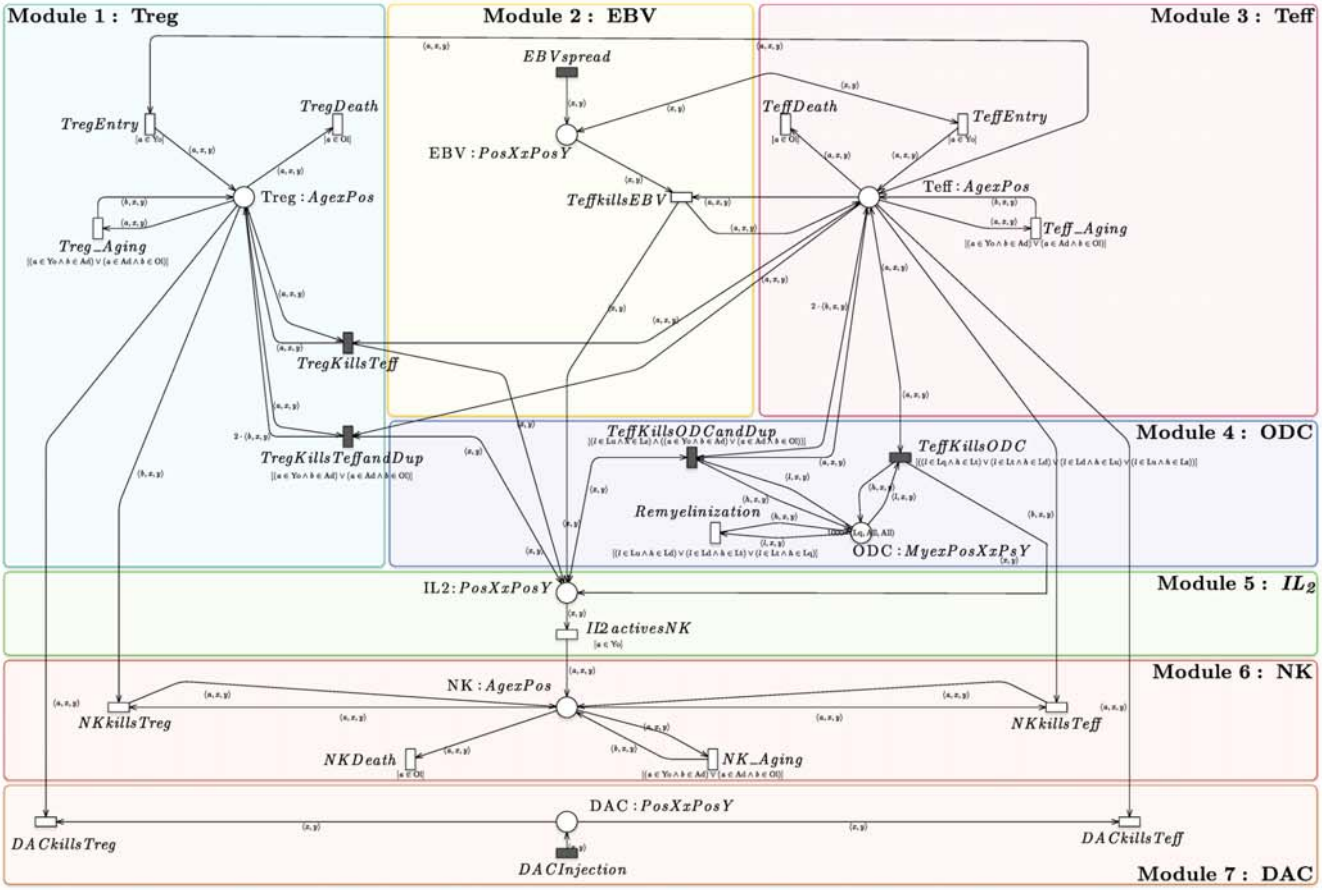

Fig. 1: RRMS model with drug administration.

immunity, namely the Natural Killer (NK) cells. Such cells can be activated by their IL-2 low affinity receptor, and can then act against self-reactive populations. It is worth to note that in some cases ODC are able to partially recover the lost myelin if the damage is not excessive.

In healthy (predisposed) patients we suppose that both Teff and Treg have similar duplication rates, so an oscillatory behavior can be observed. However this typically does not cause the insurgence of the disease. Otherwise, if a breakdown of this regulatory mechanism occurs, the Teff population may spread, having as a result neural damage.

When administered, Daclizumab (DAC) can block the T cells self-stimulating mechanisms by inhibiting their high-affinity IL-2 receptor, and thus blocking activation and duplication. This mechanism is the core of the SSN model presented in Fig. 1 and used in Section IV to investigate the effect of Daclizumab drug on RRMS.

For the sake of clarity this model is split in six modules corresponding to the main biological entities characterizing RRMS (i.e. Treg, Teff, EBV, DAC, IL2, ODC and NK).

The color classes in the model are:

- *Age* encoding the age of a cell. It is divided in three static subclasses (i.e. *YO*, *Ad*, and *Ol*) corresponding to the levels young, adult and old;
- *Mye* encoding the myelination levels of ODC. It is divided into 5 static subclasses (i.e. *Lz, Lu, Ld, Lt* and *Lq*) so that myelination level ranges from 0 (no myelination) to 4 (full myelination);
- *PosX* and *PosY* encoding the spatial coordinates of all entities in a tissue portion.

Each module is now described in details. The first module is related to Treg cells. The Place *Treg* has color domain $Age \times PosX \times PosY$, so that any Treg cell is characterized by its age and position. Transitions *TregEntry*, *TregAging* and *TregDeath* model the arrival in the system of a new activated Treg cell depending by the Teff cell number, the Treg biological aging and the Treg death respectively. Transitions *TregkillsTeff* and *TregkillsTeffandDup* model the homeostatic regulation operated by Treg cells against self-reactive Teff cells whose lead to the production of IL2. Observe that differently by *TregkillsTeff*, *TregkillsTeffandDup* introduces a Treg duplication whenever a Teff cell is killed. In this case the produced IL2 is automatically consumed by the duplication.

The second module described the EBV behaviour. The place *EBV* has color domain $PosX \times PosY$, so that any EBV is only characterized by its position. Transition *EBVspread*

Authorized licensed use limited to: University of Catania. Downloaded on June 19,2020 at 08:35:03 UTC from IEEE Xplore. Restrictions apply.

models the spreading of EBV virus in the system. *TeffkillsEBV* encodes the immunological response of Teff cells in which EBV are killed producing IL2. This interaction clearly hides the real chain of steps that goes from antigen processing and presentation by EBV infected cells to Teff cells, and that finally leads to the activation of autologus Teff cells.

Teff cells are instead described in module 3. Teff cells, as Treg cells, are characterized by their age and position; so that the color domain of place Place *Treg* is $Age \times PosX \times PosY$. The transitions *TeffEntry*, *TeffAging* and *TeffDeath* model the arrival in the system of a new activated Teff cells depending by the EBV quantity, the Teff biological aging and the Teff death respectively.

The fourth module encodes the ODC behaviour. Since ODC are described in the model through their myelination level and position, then the color domanin of place *ODE* is $Mye \times PosX \times PosY$. Transitions *TeffkillsODC* and *TeffkillsODCandDup* model the damage that Teff cells produce against ODC cells. This damage produces IL2 that in case of *TeffkillsODCandDup* is directly used to duplicate Teff cell. The remyelinization process is instead modelled by transition *Remyelinization*.

Module 5 represents the IL2 concentration in any grid cell, so that the color domanin of place *IL2* is $PosX \times PosY$. Hence, the transition *IL2activesNK* models the activation of NK cell due to IL2.

The NKs are instead modelled in the module 6. NK are described by their age and position since the domain of place *NK* is $Age \times PosX \times PosY$. The aging and death of NK is then modelled by transitions *TeffAging* and *TeffDeath* respectively. Transition *NKkillsTeff* encodes the killing of self-reactive Teff cells due to NK cells; while the transition *NKkillsTreg* the killing of Treg cells due to NK cells.

In the last module the Daclizumab behaviour is modelled through the place *DAC* with color domain $PosX \times PosY$ and the transitions *DACinjection, DACkillsTeff* and *DACkillsTreg*. The Daclizumab administration is thus modelled by transition *DACinjection*, while the pharmacokinetic killing of Treg and Teff cells is modelled by transitions *DACkillsTeff* and *DACkillsTreg*.

Finally, transitions *TregkillsTeff*, *TregkillsTeffandDup*, *EBVspread*, *TeffkillsODC*, *TeffkillsODCandDup* and *DACinjection* are modelled as general transitions because they do not follow the mass action law. In details the *EBVspread* and *DACinjection* inject into the system a specific quantities of EBV and DAC respectively at fixed time points. Differently the other two transitions depend on the probabilities of a Treg and Teff to duplicate (denoted as P_{dup}^{reg} and P_{dup}^{reg} respectively). Especially P_{dup}^{eff} is described by the Eq. 2 in which a non linear relationship with the Treg, ODC and IL2 values is modelled.

$$P_{dup}^{eff} = r_{dup} \left(\frac{ODC}{max(ODC)} \right)^2 \frac{IL2}{(1+IL2)} \left(1 - \frac{Treg}{Treg+1} \right), \quad (2)$$

where:

- r_{dup} represents the constant duplication probability, fixed to 0.1;
- $\left(\frac{ODC}{max(ODC)} \right)^2$ is a coefficient directly related to the quantity of ODC inside the area of interest. In details the value ODC is the number of ODC cells at time ν,so that an increase in the number of these cells involves an increase in the duplication probability;
- $\frac{IL2}{(1+IL2)}$ is a coefficient directly related to the quantity of IL2 in a grid position. In this way an increase in the number of these cells involves an increase in the duplication probability;
- $1 - \frac{Treg}{Treg+1}$ is instead the coefficient inversely proportional to the amount of Tregs in grid cell.

Differently the P_{dup}^{reg} is considered constant independently from the marking of the model. For more details see [7].

IV. Results

In this section we firstly present the prototype computational framework that we developed to study the RRMS, and then we report three experiments. In the first experiments the input parameters of the model are studied to characterize the difference between the behaviour of healthy and ill patients. Then two cases of different RRMS severity are considered for studying the effect of different Daclizumab administration strategies.

A. Framework Architecture

The prototype developed framework was integrated in GreatSPN [16], a well-known software suite for modelling and analyzing complex systems through the PN formalism and its extensions. The architecture of this framework is depicted in Fig. 2. The GreatSPN GUI is used to generate an SSN model, while the GreatSPN engine module is exploited to automatically derive from an SSN model the corresponding ODE system. Then, R software is utilized for solving the previously generated ODE system, and for carrying out the sensitivity analysis.

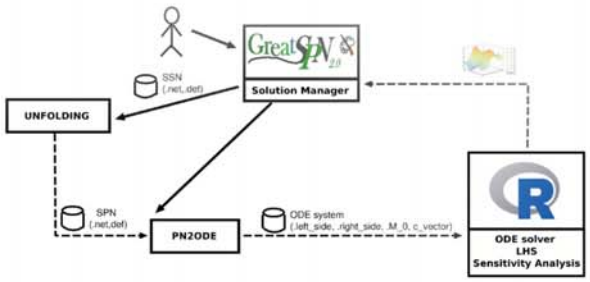

Fig. 2: Schematization of the prototype framework combining GreatSPN suite with R (the components are shown by rectangles, component invocations by solid arrows, models/data exchanges by dashed arrows).

Authorized licensed use limited to: University of Catania. Downloaded on June 19,2020 at 08:35:03 UTC from IEEE Xplore. Restrictions apply.

B. Model without drug administration

In this subsection to achieve the sensitivity analysis we consider a simpler scenario characterized by no drug injections and a grid composed by one cell. Then, the model represented in Fig. 1 (without the *DAC* place) is translated into 16 ODEs. The model input parameters are reported in the table I. Parameter values were sampled by means of LHS, in particular 4000 parameter combinations were generated using an *Uniform* distribution whose ranges are showed in the third column of the table I.

Parameters	Transition	Range
$NKbirth$	$IL2actives NK$	$[10^{-6}, 10^{-4}]$
$NKdeath$	NK_Aging & $NKDeath$	$[10^{-2}, 1]$
$NKkillTcell$	$NKkillsTreg$ & $NKkillsTeff$	$[10^{-5}, 10^{-2},]$
$ODCrec$	$Remyeinization$	$[10^{-5}, 10^{-1}]$
$TcellsDeath$	$Teff\_Aging$ & $Treg\_Aging$ $TeffDeath$ & $TregDeath$	$[10^{-6}, 10^{-3}]$
$TcellsEntry$	$TeffEntry$ & $TregEntry$	$[10^{-3}, 1]$
$TeffkillEBV$	$TeffkillsEBV$	$[10^{-2}, 1]$
$TeffkillODC$	$TeffkillsODCandDup$ with probability P^{eff}_{dup} $TeffkillsODC$ with probability $1 - P^{eff}_{dup}$	$[10^{-5}, 1]$
$TregkillTeff$	$TregkillsTeffandDup$ with probability P^{reg}_{dup} $TregkillsTeff$ with probability $1 - P^{reg}_{dup}$	$[10^{-5}, 1]$
P^{reg}_{dup}	-	$[0, 1]$

TABLE I: List of the model parameters and their corresponding ranges on whose the Uniform distribution is defined.

For lack of space in this paper we report only the result related to the *ODC* place, but similar consideration can be derived for all the other places. This place is the most important variable for the spreading of the disease indeed, starting with a value of 10000 *ODC* cells we define the disease occurrence when the lowest level of neuronal myelinization is reached for each ODC cell. This event represents an irrevirsible damage. Then, the initial marking condition of our model assumes 10000 Lq colored tokens in the place *ODC* (i.e. the Mye-subclass representing the highest level of neuronal myelinization) and zero for the other places.

In these experiments ten virus injections are simulated at irregular times, introducing into the system 1000 EBV copies per injection. From the Fig. 4a) it is straightforward to see that these injections induce an oscillatory behaviour constituted by several peaks in correspondence with each injection (see Fig. 4b) for the Teff plus Treg cells case).
Model solutions were then calculated for each parameter combination over the same one year time interval $[0, 364]$. In particular several different scenarios are identified by this analysis, such as i) the occurrence of the MS, represented by the complete elimination of the ODC cells (red lines in the Fig. 5a)), ii) the partial recovery or the no occurrence of the disease (green lines in the Fig. 5a)), iii) the total and also iv) the partial elimination of the virus (see Fig. 4a)).

Since all the ten parameters are unknown, the PRCC analysis is exploited to identify key model parameters whose mostly

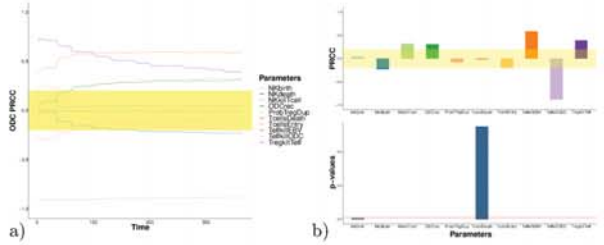

Fig. 3: *a) ODC*'s PRCCs over the whole time interval. Yellow area represents the zone of non-significant PRCC values. *b) ODC*'s PRCCs and p-values at fixed time 364.

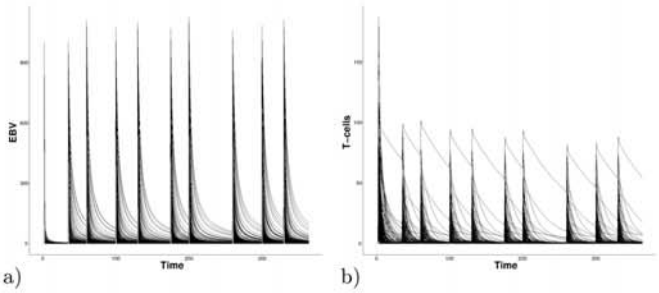

Fig. 4: A subset of the 4000 trajectories generated by LHS of the EBV cells (a) and the Teff and Treg cells (b) over the whole time interval.

affect the system behaviour. In details the PRCCs values are calculated for each parameter over the entire time period, in Fig. 3a) we report the study on the *ODC* place. In this case the *TeffKillODC* is the most important parameter that negatively affects the *ODC* behaviour (a PRCC equal to -0.8, almost steady for the whole time period, see Fig. 3). In particular this is well shown from the Fig. 5a), where all the trajectories are colored depending on the *TeffKillODC* value. Thus small values (red color) represent the occurrence of the disease while higher values (green color) a lower disease severity. Similarly in Fig. 5b), where the ODC quantity at the final time point (in the y-axis) are plotted for all the 4000 simulations varying the *TeffKillODC* parameter (in the x-axis). It is trivial to see that the increasing of this parameter leads to a decrease of the ODC value. This agrees with our expectation since this parameter represents how rapidly a Teff kills an ODC.

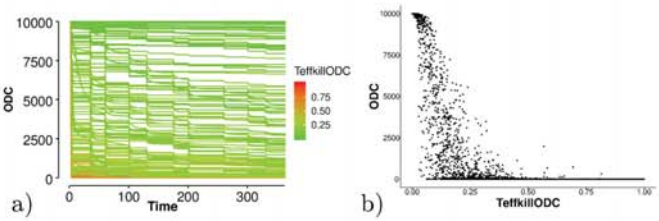

Fig. 5: a) ODC trajectories over the whole time interval colored depending on the *TeffkillODC* parameter value. b) Scatter plot of the ODC variable at the fixed time 364 versus the *TeffkillODC* parameter variation.

Authorized licensed use limited to: University of Catania. Downloaded on June 19,2020 at 08:35:03 UTC from IEEE Xplore. Restrictions apply.

ProbTregDup	TcellsEntry	TcellsDeath	TeffkillEBV	TregkillTeff	TeffkillODC	ODCrec	NKbirth	NKdeath	NKkillTcell	DAC	DACkillTcell
0.0999211126	0.5471441357	0.0071075847	0.4092896089	0.7009959135	0.1207079396	0.9932666685	0.0009100245	0.1679735563	0.0415897458	[100, 500]	$[10^{-4}, 1]$
0.6606498798	0.5079247409	0.0020994473	0.8848492579	0.2334677852	0.4285406660	0.9230286051	0.0008853756	0.6935743292	0.0762275166	[100, 500]	$[10^{-4}, 1]$

TABLE II: Parameters used for simulating the weak version (first row) and strong version (second row) of the disease.

C. Model with drug administration

We extrapolate from the experiments described in the previous subsection two parameters combinations representing two specific scenarios. The first set of parameters leads to a weak occurrence of the disease (just an half of the *ODC* are eliminated). Differently with the second combination a strong version of the disease is represented (all the *ODC* are almost eliminated). In details the parameters values modeling these two scenarios are reported in the Table II, where the parameters value depicting the weak version of the disease are reported in the first row, and the ones representing the strong version in the second row.
Selected these two cases, we simulate the Daclizumab therapy starting at time 60. This therapy consists in a *DAC* injection per month, where the quantity of *DAC* administrated per injection is sampled by means of LHS using an *Uniform* distribution. With the same strategy the *DACkillTcell* parameter, representing the rate with which a *DAC* cell kills a Treg or a Teff cell, is generated. The ranges on which these two Uniform distributions are defined are reported into the last two columns of the Table II.

Figs. 6 and 7 show how much the trajectories representing the ODC, the Treg and Teff (two of the main actors of the immune mechanisms involved in the development of the disease), and the IL2 (that promotes T cells actions) vary after the drug administration. In particular it is possible to see (Figs. 6a and 7a) that an increasing DAC quantity has a positive effect on the number of ODC cells that tends to be higher with increasing DAC quantities. However, as it is possible to see from Fig. 7a, when the severity of the disease is very high, the drug efficacy is weak, thus leading to a worsening of the disease. The described scenario can be better observed in in Fig. 7b, where a logarithmic scale on the y-axis is used. This is due to the fact that an irreversible damage, from which is not possible to recover, already holds from the beginning of the experiment for the majority of the *ODC*.
In Figs. 6c, 6e and Figs. 7c, 7e the Treg and Teff, and the IL2 quantities variations are shown. In particular in both the cases under study it is possible to observe a more relevant decreasing of these quantities, as more DAC is injected. This reflects the effect of the drug, that inhibits Teff and Treg actions, responsible of the neural damage. Interestingly, in the more severe scenario such quantities are lower. This may be due to the lower quantities of IL2 observed in the worst case scenario. IL2 is released to self-stimulate duplication of Teff and Treg cells as a consequence of a succefull interaction (i.e., Teff kills ODC). If the number of ODC is very low (as already stated in this case of study) the probability for Teff to interact with ODC will be lower and, therefore, also the release of IL2 will be influenced.

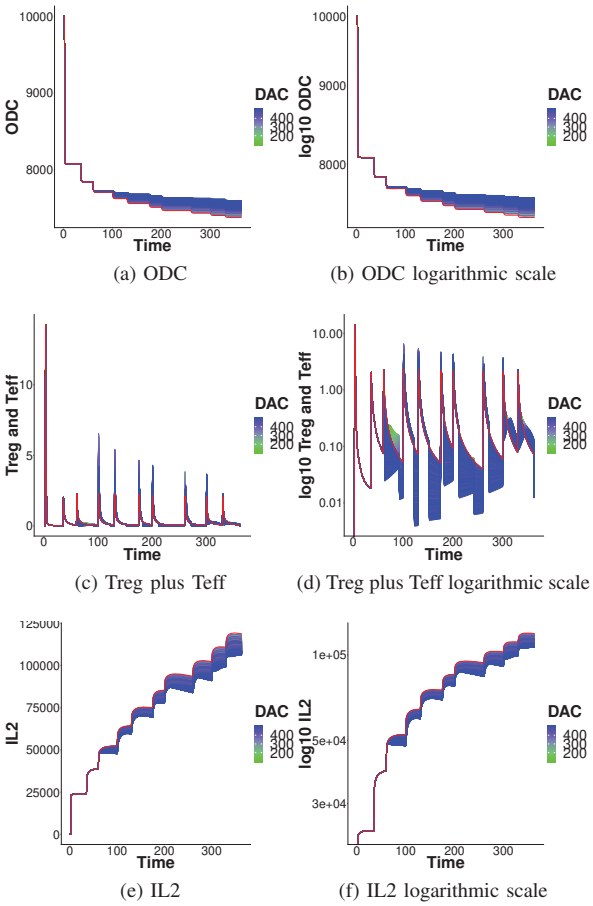

(a) ODC (b) ODC logarithmic scale
(c) Treg plus Teff (d) Treg plus Teff logarithmic scale
(e) IL2 (f) IL2 logarithmic scale

Fig. 6: First case representing the weak disease. *ODC*, *Treg* plus *Teff* and *IL2* trajectories colored depending on *DAC* quantity administrated. The red line represents the starting sample without drug administration.

It is worth to note here that the DAC inhibition will affect not only the self-reactive T cells observed here, but the whole T cells populations, and in particular all Treg cells that are fundamental to protect ourselves from autoimmune diseases. Beyond that, recent studies have also shown how Tregs, when further stimulated with low IL-2 dosages, can be protective in the development of autoimmune diseases such as autoimmune encephalitis [17].

Thus, the lower number of Teff and Treg and lower the quantity of IL2 observed for both the scenarios in which the DAC is administered (in respect to the untreated case) may represent the motivations that lead to the occurring of the aforecited adverse effects.

Authorized licensed use limited to: University of Catania. Downloaded on June 19,2020 at 08:35:03 UTC from IEEE Xplore. Restrictions apply.

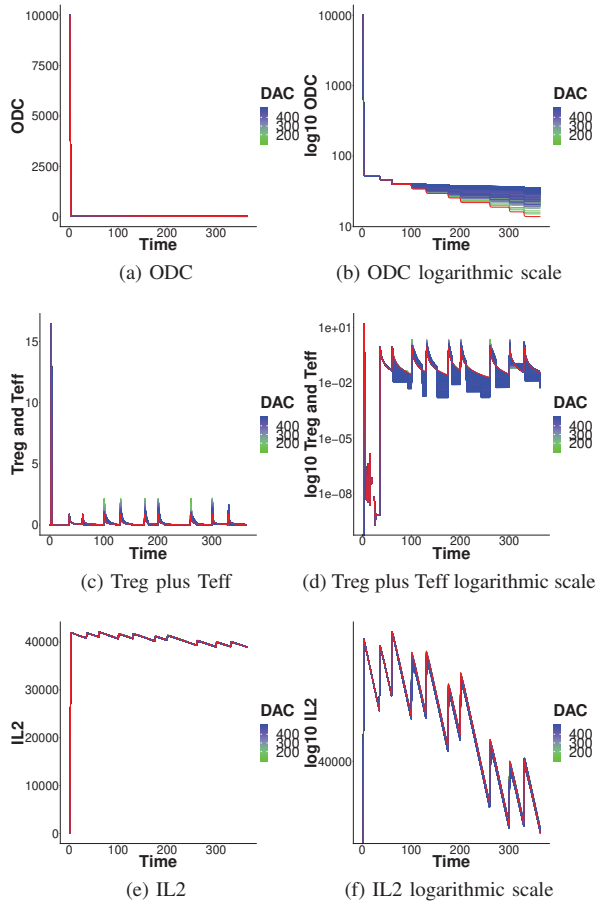

(a) ODC (b) ODC logarithmic scale

(c) Treg plus Teff (d) Treg plus Teff logarithmic scale

(e) IL2 (f) IL2 logarithmic scale

Fig. 7: Second case representing the strong disease. *ODC*, *Treg* plus *Teff* and *IL2* trajectories colored depending on *DAC* quantity administrated. The red line represents the starting sample without drug administration.

V. Conclusion and Future Perspective

In this paper we presented a novel computational model for the analysis of the RRMS with the Daclizumab administration. In particular the descriptive power of Stochastic Symmetric Nets is exploited to provide a graphical representation of a complex biological system in a compact and parametric way. Then we showed that the model is able to reproduce the typical oscillatory behavior that relates to the onset of relapsing remitting MS by supposing a breakdown of the cross-balance regulation mechanisms at the peripheral level. Furthermore, it allowed one to grasp the mechanisms of actions of Daclizumab and to theorize the possible causes of the observed side-effect on the patient health.

A future work will be to deeply investigate all those model parameters associated with low PRCC value and p-value because this could indicate non linear and/or non-monotone relationships which are not captured by the PRCC approach. Moreover, we will extend our analysis to consider a greater grid.

References

[1] Dutta, R., Trapp, B.D.: Mechanisms of Neuronal Dysfunction and Degeneration in Multiple Sclerosis. Prog. Neurobiol. **93**(1), 1–12 (2011)

[2] Trapp, B.D., Nave, K.-A.: Multiple Sclerosis: An Immune or Neurodegenerative Disorder? Annu. Rev. Neurosci. (2008). NIHMS150003

[3] Clerico, M., Artusi, C.A., Di Liberto, A., Rolla, S., Bardina, V., Barbero, P., De Mercanti, S.F., Durelli, L.: Natalizumab in Multiple Sclerosis: Long-Term Management. Int. J. Mol. Sci. **18**(5), 940 (2017)

[4] Salzer, J., Svenningsson, R., Alping, P., Novakova, L., Björck, A., Fink, K., Islam-Jakobsson, P., Malmeström, C., Axelsson, M., Vågberg, M., Sundström, P., Lycke, J., Piehl, F., Svenningsson, A.: Rituximab in multiple sclerosis: A retrospective observational study on safety and efficacy. Neurology **87**(20), 2074–2081 (2016)

[5] Guarnera, C., Bramanti, P., Mazzon, E.: Alemtuzumab: a review of efficacy and risks in the treatment of relapsing remitting multiple sclerosis. Ther. Clin. Risk Manag. **13**, 871–879 (2017)

[6] Wynn, D., Kaufman, M., Montalban, X., Vollmer, T., Simon, J., Elkins, J., O'Neill, G., Neyer, L., Sheridan, J., Wang, C., Fong, A., Rose, J.W.: Daclizumab in active relapsing multiple sclerosis (CHOICE study): a phase 2, randomised, double-blind, placebo-controlled, add-on trial with interferon beta. Lancet Neurol. **9**(4), 381–390 (2010)

[7] Pennisi, M., Rajput, A.M., Toldo, L., Pappalardo, F.: Agent based modeling of treg-teff cross regulation in relapsing-remitting multiple sclerosis. In: BMC Bioinformatics (2013)

[8] Beccuti, M., Cazzaniga, P., Pennisi, M., Besozzi, D., Nobile, M.S. S. Pernice, Russo, G., Tangherloni, A., F., P.: Gpu accelerated analysis of treg-teff cross regulation in relapsing-remitting multiple sclerosis. In: 4th International European Conference on Parallel and Distributed Computing (Euro-Par 2018). LNCS. Springer, ??? (2018)

[9] Chiola, G., Dutheillet, C., Franceschinis, G., Haddad, S.: Stochastic well-formed coloured nets for symmetric modelling applications. IEEE Transactions on Computers **42**(11), 1343–1360 (1993)

[10] Marsan, M.A., Balbo, G., Conte, G., Donatelli, S., Franceschinis, G.: Modelling with Generalized Stochastic Petri Nets. J. Wiley, New York, NY, USA (1995)

[11] Kurtz, T.G.: Strong approximation theorems for density dependent Markov chains. Stoc. Proc. Appl. **6**(3), 223–240 (1978)

[12] Beccuti, M., Fornari, C., Franceschinis, G., Halawani, S.M., Ba-Rukab, O., Ahmad, A.R., Balbo, G.: From symmetric nets to differential equations exploiting model symmetries. Computer Journal **58**(1), 23–39 (2015)

[13] Marino, S., Hogue, I.B., Ray, C.J., Kirschner, D.E.: A methodology for performing global uncertainty and sensitivity analysis in systems biology. Journal of Theoretical Biology **254**(1), 178–196 (2008)

[14] Saltelli, A., Ratto, M., Tarantola, S., Campolongo, F.: Sensitivity analysis for chemical models. Chemical Reviews **105**(7), 2811–2828 (2005)

[15] McKay, M.D., Beckman, R.J., Conover, W.J.: A comparison of three methods for selecting values of input variables in the analysis of output from a computer code. Technometrics **21**(2), 239–245 (1979)

[16] Babar, J., Beccuti, M., Donatelli, S., Miner, A.S.: GreatSPN enhanced with decision diagram data structures. In: Lilius, J., Penczek, W. (eds.) Application and Theory of Petri Nets. PETRI NETS 2010. LNCS, vol. 6128, pp. 308–317. Springer, ??? (2010)

[17] Lim, J.A., Lee, S.T., Moon, J., Jun, J.S., su Park, B., Byun, J.I., Sunwoo, J.S., Park, K.I., Jung, K.H., Jung, K.Y., Lee, S.K., Chu, K.: New feasible treatment for refractory autoimmune encephalitis: Low-dose interleukin-2. J. Neuroimmunol. (2016)

Authorized licensed use limited to: University of Catania. Downloaded on June 19,2020 at 08:35:03 UTC from IEEE Xplore. Restrictions apply.